Published in final edited form as:
Chem Res Toxicol. 2012 July 16; 25(7): 1402–1411. doi:10.1021/tx200513t.

DNA Damage Caused by Metal Nanoparticles: the Involvement of Oxidative Stress and Activation of ATM

Rong Wan[*,1], **Yiqun Mo**[*,1], **Lingfang Feng**[1], **Sufan Chien**[2], **David J. Tollerud**[1], and **Qunwei Zhang**[1]

[1]Department of Environmental and Occupational Health Sciences, School of Public Health and Information Sciences, University of Louisville, Louisville, KY, USA

[2]Department of Surgery, School of Medicine, University of Louisville, Louisville, KY, USA

Abstract

Nanotechnology is a fast growing emerging field, the benefits of which are widely publicized. Our current knowledge of the health effects of metal nanoparticles such as nano-sized cobalt (Nano-Co) and titanium dioxide (Nano-TiO_2) is limited but suggests that metal nanoparticles may exert more adverse pulmonary effects as compared with standard-sized particles. To investigate metal nanoparticle-induced genotoxic effects and the potential underlying mechanisms, human lung epithelial cell lines A549 cells were exposed to Nano-Co and Nano-TiO_2. Our results showed that exposure of A549 cells to Nano-Co caused reactive oxygen species (ROS) generation that was abolished by pretreatment of cells with ROS inhibitors or scavengers, such as catalase and N-acetyl-L(+)-cysteine (NAC). However, exposure of A549 cells to Nano-TiO_2 did not cause ROS generation. Nano-Co caused DNA damage in A549 cells which was reflected by an increase in length, width, and DNA content of the comet tail by Comet assay. Exposure of A549 cells to Nano-Co also caused a dose-and a time- response increased expression of phosphorylated histone H2AX (γ-H2AX), Rad51 and phosphorylated p53. These effects were significantly attenuated when A549 cells were pre-treated with catalase or NAC. Nano-TiO_2 did not show these effects. These results suggest that oxidative stress may be involved in Nano-Co-induced DNA damage. To further investigate the pathways involved in the Nano-Co-induced DNA damage, we measured the phosphorylation of ataxia telangiectasia mutant (ATM). Our results showed that phosphorylation of ATM was increased when A549 cells were exposed to Nano-Co, and this effect was attenuated when cells were pretreated with catalase or NAC. Pre-treatment of A549 cells with an ATM specific inhibitor, KU55933, significantly abolished Nano-Co-induced DNA damage. Furthermore, pre-treatment of A549 cells with ROS scavengers, such as catalase and NAC, significantly abolished Nano-Co-induced increased expression of phosphorylated ATM. Taken together, oxidative stress and ATM activation are involved in Nano-Co-induced DNA damage. These findings have important implications for understanding the potential health effects of metal nanoparticle exposure.

Keywords

metal nanoparticles; DNA damage; ROS; histone H2AX phosphorylation; p53; activation of ATM; A549 cells

Address Correspondence To: Qunwei Zhang, MD, MPH, PhD, Department of Environmental Health and Occupational Health Sciences, School of Public Health and Information Sciences, University of Louisville, 485 E. Gray Street, Louisville, KY 40202, Tel: (502)852-7200, Fax: (502)852-7246, Qunwei.Zhang@louisville.edu.

*R. Wan and Y. Mo contributed equally to this work.

The results were presented in part at 2010 American Thoracic Society (ATS) International Conference; May 14–19, 2010; New Orleans, LA.

Introduction

The increased development and use of nanoparticles for various industries could lead to increased exposure, affecting human health and the environment.[1–3] For example, metal nanoparticles are widely used in cosmetics, medicine, electronics and industry. Therefore, occupational or non-occupational exposure to metal nanoparticles is growing. Our current knowledge of the potential health effects of nanomaterials is limited but suggests that they may exert adverse effects at their portal of entry, such as lung, skin and gastrointestinal tract.[1, 4–5] In addition, some nanomaterials may have genotoxic or carcinogenic effects because of the certain metals used to make them. Some metal particles can lead to reactive oxygen species (ROS) generation that causes oxidative stress and DNA damage in the body.[6–7] Although some studies have shown the potential genotoxic effects of some nanomaterials,[8–9] the mechanisms are still unclear. In this study, we selected Nano-Co as a 'model' metal nanoparticle because of its industrial interest and wide biological and medical applications. We examined its potential genotoxic effects and the possible mechanisms involved. Metallic cobalt, as nanoparticles, is used in biology and medicine in different forms from the simplest, such as cobalt oxide, to complex, such as organic compounds or biopolymers.[10–11]

It is well-known that one initiating pathogenic effect of oxidative stress is inflammation, which can cause DNA damage and genotoxicity.[6–7, 12–13] The association between genotoxicity and cancer is also well known. For example, the carcinogenic effects of ionizing radiation, UV radiation and many chemical carcinogens are based on their ability to cause DNA damage and consequent gene mutation.[6, 14] There are several excellent reviews regarding metals, oxidative stress and cancer.[6, 13, 15–16] It is generally accepted that excessive generation of ROS that overwhelms the antioxidant defense system can oxidize cellular biomolecules.[7] Free radicals also cause oxidative modifications in DNA, including strand breaks and base oxidation. Among oxidative DNA damage products, 8-hydroxy-2'- -deoxyguanosine (8-OHdG) is probably the most studied, due to its relative ease of measurement and pre-mutagenic potential.[6–7, 13–14] Elevated 8-OHdG has also been noted in numerous tumors, strongly implicating such damage in the etiology of cancer.[7, 14]

The p53 protein is regarded as a master guardian of the cell and is able to activate cell cycle checkpoint, DNA repair, and apoptosis response to maintain genomic stability.[8–9] In the absence of a stress insult, such as DNA damage, p53 is kept in low concentration at the cell by rapid degradation via the ubiquitin pathway.[8–9] However, in the present of DNA damage, p53 accumulates and triggers cell cycle arrest to provide time for the damage to be repaired.[17–19] In response to a variety of cellular stresses, p53 protein is phosphorylated on multiple residues in both the amino- and carboxy-terminal domains by several different protein kinases.[20–21] Among the serine residues, phosphorylation at Ser 15 has been shown to be responsible for the stabilization, subsequent induction and transactivation function of p53. In addition, phosphorylation of mouse p53 at Ser 18 (corresponding to Ser 15 of human p53) is required for maximum p53-mediated response to DNA damage.[17, 19]

The ataxia telangiectasia mutated (ATM) protein, encoded by the gene responsible for the human genetic disorder ataxia telangiectasia (A-T), regulates several cellular responses to DNA breaks.[16, 20–22] The activation of ATM results in the phosphorylation of a plethora of downstream targets. Some of these proteins are direct substrates of ATM. For example, ATM likely directly phosphorylates Ser 15 of p53 and Ser 139 of histone H2AX in response to DNA damage.[21–22] Others may be phosphorylated indirectly, through ATM-mediated regulation of other protein kinases, such as Chk1, Chk2 and IκB kinases.[20] To date, most studies have examined the effects of ionizing radiation (IR) on the activation of ATM and

ATM-dependent downstream pathways.[20, 22] Only a few studies have focused on the role of activation of ATM and p53 in metal nanoparticle-induced DNA damage.

In the present study, human lung epithelial cell line A549 was selected as a model cell line since inhalation is the most important route of occupational and environmental exposure to cobalt and its compounds.[23–24] We first investigated whether exposure of A549 cells to Nano-Co or Nano-TiO_2 resulted in DNA damage. Then we explored the potential mechanisms involved in these effects. We propose that exposure of human lung epithelial A549 cells to non-toxic doses of Nano-Co will cause ROS generation, which may further result in DNA damage through activation of ATM pathway.

Results and Discussion

Cytotoxic effects of Nano-Co or Nano-TiO_2 on A549 cells

The effects of different concentrations (0–40 μg/ml) of Nano-Co or Nano-TiO_2 on A549 cells were assessed by both the colorimetric SRB assay and the fluorescent AlamarBlue™ assay. Fig. 1 showed that no significant cytotoxicity was observed when cells were exposed to 15 μg/ml or less concentrations of Nano-Co for 24 h by both methods. However, exposure of A549 cells to 20 μg/ml and above of Nano-Co caused significant cytotoxicity. In contrast, exposure to Nano-TiO_2 did not cause any significant cytotoxic effects at all experimental dose points. Non-toxic doses were selected for the subsequent experiments. Several factors may affect cytotoxicity of nanoparticles such as small diameter, high surface area, and the chemical composition.[2, 4] Although Co ions may be released from Nano-Co into the medium, previous studies showed that exposure of cells to the same amount of cobalt in ionic form did not cause cytotoxic effects.[25] It is difficult to estimate the degree of human health effects that might occur at such non-toxic concentrations or quantity of Nano-Co. However, using doses that are lower than the cytotoxic dose can help identify potential health effects of Nano-Co other than those due to cytotoxicity.

Uptake of metal nanoparticles by A549 cells

A549 cells were treated with 5 or 15 μg/ml of Nano-TiO_2 or Nano-Co for 12 h. The uptake of Nano-TiO_2 or Nano-Co by A549 cells were measured by ICP-MS. Our results showed that the uptake of Nano-Co was 4.21×10^{-12} and 8.33×10^{-12} (g/cell) with exposure to 5 and 15 μg/ml of Nano-Co respectively. It was 2.75×10^{-12} and 4.34×10^{-12} (g/cell) with exposure to 5 and 15 μg/ml of Nano-TiO_2. Our results indicated that there was a clear dose-dependent uptake of metal nanoparticles by A549 cells. The amount of metal nanoparticle uptake was correlated directly with the concentration of metal nanoparticles in the extracellular solution. These results suggest that nanoparticle concentration within the cell culture medium can provide a relatively accurate measurement of the nanoparticle dose delivered to the cell surface.

Exposure of A549 cells to Nano-Co, but not to Nano-TiO_2, caused ROS generation and increase of 8-OHdG level

Oxidative stress is considered to be an important mechanism for particle-induced health effects. Exposure to some types of nanoparticles induces oxidative stress in cells, and activation of oxidative stress-responsive transcription factors such as NF-κB and AP-1, together with the depletion of antioxidant defenses, can lead to the release of proinflammatory cytokines.[2, 5, 8–9] It is generally accepted that oxidative stress eventually causes DNA damage, which plays an important role in the development of carcinogenesis.[26] To examine whether exposure to Nano-Co caused ROS generation, we used a fluogenic probe 2',7'-dichlorodihydrofluorescein diacetate (H_2-DCFDA) to measure ROS generation in A549 cells with exposure to Nano-Co. H_2-DCFDA is a colorless and non-fluorescent

"dihydro" derivative of fluorescein. However, its oxidation to the parent dye provides the basis for it to serve as a fluorogenic probe for the detection of ROS, including H_2O_2. In additional, 8-OHdG is a representative oxidative product of guanine and a highly mutagenic lesion that causes mispairing of 8-OHdG with deoxyadenosine (dA). It is a good marker for oxidative stress - induced DNA damage. Our results showed that exposure of A549 cells to Nano-Co caused a dose-dependent increase in ROS generation reflected by an increase in DCF fluorescence (Fig. 2A) and increased level of 8-OHdG in genomic DNA (Fig. 2B). However, exposure to the same concentrations of Nano-TiO_2 did not cause an increase in either DCF fluorescence or 8-OHdG level in genomic DNA (Fig. 2 A& B). Further, pre-treatment of cells with ROS scavengers NAC (10 mM) or catalase (2,000 U/ml) prior to Nano-Co treatment markedly attenuated Nano-Co-induced ROS generation (Fig. 2C). These results suggested that cells exposed to Nano-Co caused ROS generation.

Nano-Co induced DNA damage in A549 cells

Although there is still controversy regarding the genotoxicity of metal cobalt particles, cobalt ion has been shown to have genotoxic effects both *in vitro* and *in vivo*.[23, 27] The comet assay is a sensitive and rapid method for detecting DNA single- and double-strand breaks at individual cells.[28] Cells that have broken DNA fragments or damaged DNA migrate much further and appear as fluorescent comets with tails of DNA fragmentation or unwinding, whereas intact undamaged DNA moves minimally due to its large size. Our comet assay results showed that there was a dose-response increase in DNA damage after exposure of A549 cells to 0, 5 and 15 μg/ml of Nano-Co, whereas Nano-TiO_2 did not induce any significant DNA damage (Fig. 3A). Our results also showed a time-response increase in DNA damage in A549 cells exposed to Nano-Co for 12 to 48 h (data not shown). Again, Nano-TiO_2 did not cause a time-response increase in DNA damage (data not shown). These results were consistent with previous studies showing that exposure to Nano-Co caused DNA damage in human peripheral leukocytes or mouse Balb/3T3 fibroblasts by comet assay.[25, 29] Oxidative stress is thought to be responsible for the genotoxic effects exerted by various nanomaterials.[8] To examine whether Nano-Co-induced DNA damage through oxidative stress, A549 cells were pre-treated with ROS inhibitors or scavengers, such as NAC (10 mM) or catalase (2,000 U/ml) for 2 h prior to 15 μg/ml of Nano-Co treatment for another 12 h. The results showed that Nano-Co-induced DNA damage was significantly attenuated when A549 cells were pre-treated with NAC or catalase (Fig. 3B). These results indicated that Nano-Co-induced ROS generation was involved in Nano-Co-induced DNA damage. Although it is difficult to identify whether ROS generation and DNA damage in A549 cells is through Nano-Co itself or Co^{2+} released from Nano-Co, our results in table 2 showed that the Co ion concentration in the medium was very low (about 45.35 ppm). Previous studies reported that such low concentration of Co ion did not cause any DNA damage in cells.[25, 29]

Nano-Co induced DNA double strand breaks (DSBs)

In humans and other eukaryotes, DNA is wrapped around histone-groups, consisting of core histones H2A, H2B, H3 and H4. H2AX contributes to histone-formation and therefore the structure of DNA.[31] It is well known that repair mechanisms for a specific type of DNA damage, such as DSB involve the phosphorylation of H2AX.[32] Since H2AX phosphorylation at Ser 139 correlates very closely with each DSB break, phospho-H2AX (γ-H2AX) is a sensitive marker for DNA damage and can be used to assess the effects and timing of DNA damage-inducing and DNA repair agents. Therefore, the presence of γ-H2AX is a sensitive biomarker of DNA damage and these sites can be detected by immunofluorescence microscopy utilizing fluorescently labeled antibodies specific to γ-H2AX.[32–33] In this study, we first assessed γ-H2AX to monitor the induction of DSBs after exposure to Nano-Co or Nano-TiO_2 by using immunofluorescence staining. The results

showed that there was a dose-response increase in the formation of γ-H2AX foci in A549 cells with exposure to Nano-Co (Fig. 4A).

To further examine whether exposure Nano-Co-induced DNA DSBs, we also determined the phosphorylation of H2AX expression by using western blot method. The results were consistent with the immunofluorescence results (Fig. 5 A&B). Our results also demonstrated a time-response increase in the formation of γ-H2AX foci or expression of γ-H2AX protein when A549 cells were exposed to 15 μg/ml of Nano-Co for 0 to 24 h (Fig. 4B, 5C & 5D). However, Nano-TiO_2 did not cause an increase in either the formation of γ-H2AX foci or expression of γ-H2AX protein (Fig. 4A, 5A & 5B). Our results clearly show the dose-and time- response increases in γ-H2AX foci formation and phosphorylation of H2AX in the A549 cells with exposure to Nano-Co. These results are confirmed the comet assay results and provided a strong evidence that exposure to Nano-Co induced DNA DSB *in vitro*. Although the exact nature of Nano-Co- induced γ-H2AX foci formation is not yet clear, previous studies showed that ROS and 8-OHdG in the DNA replication stage and lipid peroxidation were involved in γ-H2AX foci formation.[31–34]

Expression of Nano-Co-induced DNA damage repair protein Rad51

Besides functioning as a biomarker for DSBs, γH2AX also helps recruit many other proteins involved in DNA damage sensing and repair, such as the Mre11/Rad50/Nbs1 (MRN) complex, BRCA1, 53BP1, etc., to form multiple protein complexes (termed foci) at the damaged site.[34] When cells are exposed to genotoxic treatments, such as UV irradiation, ionizing radiation, or mitomycin C, the Rad51 protein relocalizes and concentrates in nuclear foci that are believed to be the sites of repair.[26] Thus, the regulation of Rad51 is likely to control genomic stability in eukaryotic cell responses to various DNA-damage agents. Rad51 is an important DNA damage repair protein, which plays a major role in homologous recombination of DNA during double strand break repair.[26] To further investigate Nano-Co-induced breakdown of double stranded DNA, we assayed the other key double strand break repair protein, Rad51, by western blot. Our results showed that there was a dose- and a time- response increase in the expression of Rad51 in A549 cells exposed to Nano-Co (Fig. 5 A&B). However, treatment with Nano-TiO_2 did not cause the above effects (Fig. 5 A&B). These results also provided evidence to support our hypothesis that exposure to Nano-Co causes DNA damage.

Nano-Co induced accumulation of p53 and phosphorylation of p53 at Ser 15

P53 is a tumor suppressor gene that has a diverse range of functions that include regulation of cell cycle checkpoints, apoptosis, senescence, DNA repair, and maintenance of genomic integrity and control of angiogenesis. P53 can be activated in response to a number of cellular stressors, and it can further regulate the transcription of genes associated cell cycle control, DNA repair and apoptosis. After DNA damage, the amount of p53 in cells increases through posttranscriptional mechanisms, and its transactivation activity is enhanced, leading to the activation of downstream genes.[16] Ser 15 on p53 is a functionally important residue within the p53 amino-terminal region, and phosphorylation of Ser 15 represents an early cellular response to a variety of genotoxic stress.[35–36] To investigate whether exposure to Nano-Co resulted in accumulation of p53 and increased phosphorylation of p53 at Ser 15, we isolated nuclear protein from A549 cells exposed to Nano-Co and then performed Western blot. Our results showed that there was a dose- and a time- response increase in the p53 protein and phosphorylation of p53 at Ser 15 after A549 cells were exposed to 0, 5, 10 and 15 μg/ml of Nano-Co for 12 h (Fig. 5 A&B) or exposed to 15 μg/ml of Nano-Co for 0, 3, 6, 12 and 24 h (Fig. 5 C&D). However, exposure of A549 cells to Nano-TiO_2 did not cause any accumulation of p53 protein and increased phosphorylation of p53 at Ser 15 (Fig. 5 A&B).

Nano-Co-induced activation of ATM and the role of activation of the ATM pathway in Nano-Co-induced increased p53 at Ser 15 phosphorylation and p53 and Rad51 expression

It is believed that autophosphorylation of ATM protein at Ser 1981 is a sensitive, specific marker of DSB, and controls cellular responses to DNA damage through the phosphorylation of effecter proteins, such as p53 and H2AX.[37–38] Therefore, we investigated whether Nano-Co induced ATM activation and whether activation of ATM was involved in the Nano-Co-induced DNA damage. Our results showed that exposure of A549 cells to Nano-Co led to increased phosphorylation of ATM at Ser 1981. The level of phosphorylated ATM increased significantly in a dose-dependent manner as compared to untreated or Nano-TiO_2-treated cells (Fig. 6A). When cells were treated with 15 μg/ml of Nano-Co, the level of phosphorylated ATM at Ser 1981 was up-regulated as early as after 3 h treatment and became more distinct as the incubation time increased (Fig. 6B). In contrast, the level of total ATM was not significantly affected by exposure to either Nano-Co or Nano-TiO_2 (Fig. 6 A&B). ATM is a Ser/Thr protein kinase that is activated in response to DNA DSB and can phosphorylate multiple substrates involved in cell cycle checkpoint control and DNA repair. Activation of ATM can increase phosphorylated p53 at Ser 15, which increases its stabilization and nuclear accumulation as well as its transactivation.[20] Exposure to Nano-Co caused a rapid ATM phosphorylation at Ser 1981 and subsequently resulted in phosphorylation of p53 at Ser 15.

To further clarify whether ATM signaling was involved in the Nano-Co-induced DNA damage, a specific inhibitor of ATM, KU55933 (10 μM), was used to treat A549 cells for 1 h prior to treatment with Nano-Co for another 6 or 12h. Pre-treatment of A549 cells with KU55933 suppressed Nano-Co-induced p53 accumulation and the levels of phospho-p53 and Rad51 expression (Fig. 7A&B). These results were consistent with previous reports of IR-induced cell cycle stage-specificity of ATM activation and p53 at Ser 15 phosphorylation.[39] Our results suggested that activation of ATM may be involved in Nano-Co-induced DNA damage.

Effects of oxidative stress on Nano-Co-induced phosphorylation of ATM and p53, and increased expression of Rad51 and p53

ROS have been implicated in the phosphorylation p53 that is mediated by protein kinases, including p38 MAPK, ATM and ERK. The kinases responsible for the phosphorylation of H2AX have also been investigated, and it is now clear that H2AX phosphorylation depends on the activation of members of the phosphatidylinositol 3-kinase family (PI3K), including ATM, ATR (ATM and Rad3-related), and DNA-PK (DNA-dependent protein kinase). To explore the potential implication of oxidative stress in the DNA damage induced by Nano-Co exposure, A549 cells were pre-treated with antioxidants catalase (2,000 U/ml) or NAC (10mM) for 2 h before exposure to Nano-Co for another 12 h. Our results demonstrated that the phosphorylation of ATM and p53 and the increased expression of Rad51 and p53 induced by Nano-Co were prevented to a large extent by pre-treatment with NAC or catalase (Fig. 8 A&B). These findings suggested that Nano-Co-induced ROS generation was followed by phosphorylation of ATM and p53 and increased Rad51 expression in A549 cells. Nano-Co-induced DNA damage appears to be mediated through ROS-dependent ATM signaling pathway.

Conclusion

Taken together, our study demonstrated that exposure to non-toxic doses of Nano-Co caused oxidative stress, which further resulted in DNA damage. Nano-Co-induced DNA damage may further activate ATM pathway and increase the phophorylation of p53 and Rad 51 protein expression (Fig. 9). DNA damage can invoke various cellular responses such as cell

cycle arrest, apoptosis and importantly, DNA repair. For the DNA damage, DSBs are considered to be among the most lethal forms of DNA damage, severely compromising genomic stability. Phosphorylation of H2AX event is one of the most well-established chromatin modifications linked to DNA damage and repair. Our results suggest that the rapid phosphorylation of H2AX is an early cellular response to Nano-Co-induced DNA damage. Nano-Co-induced DNA damage is a complex process and many signaling pathways are involved in these processes, such as p-ATM, p-p53 and Rad 51. ATM acts as a sensor of ROS and oxidative damage of DNA. In turn, ATM induces signaling through multiple pathways, thereby coordinating acute phase response with cell cycle checkpoint control and repair of oxidative stress. p53 is a key effector molecule that is activated by Nano-Co-induced DNA damage while Rad 51 may be involved in assisting in repair of Nano-Co-induced DNA DSBs. These results provide further understanding of the potential genotoxic effects of metal nanoparticle exposure. However, the genotoxic effects of Nano-Co need to be further investigated since the consequences of long-term and low doses of Nano-Co exposure are still unclear.

Materials and Methods

Metal nanoparticles

Nano-Co and Nano-TiO_2 with a mean diameter of 20 nm and 28 nm were provided by INABTA and Co., Ltd., Vacuum Metallurgical Co., Ltd., Japan. The nanostructure and composition of Nano-Co and Nano-TiO_2 were characterized by transmission electron microscopy (TEM) (Hitach H-8000) and ancillary techniques including selected area electron diffraction (SAED) and energy-dispersive (X-ray) spectrometry (EDS). Nano-Co and Nano-TiO_2 were dispersed in physiological saline and ultrasonicated for 30 min prior to each experiment. The characterization of these nanoparticles has been summarized in Table 1. Briefly, the specific surface area is 47.9 m^2/g for Nano-Co and 45.0 m^2/g for Nano-TiO_2. Nano-Co is composed of 85–90% metal cobalt and 10–15% Co_3O_4; Nano-TiO_2 is composed of 90% anatase and 10% rutile. The size of particles and agglomerates in cell culture medium was 260 nm for Nano-Co and 280 nm for Nano-TiO_2, measured by dynamic light scattering (DLS).

The solubility of Nano-Co and Nano-TiO_2 in PBS and cell culture medium was measured as previously reported.[40–41] In brief, five 30 mg samples of Nano-Co or Nano-TiO_2 were suspended in 30 ml of 1 × PBS or Ham's F-12 medium in 50 ml polyethylene tubes, respectively. After shaking for 48 hrs in a water bath at 37 °C, they were ultrasonicated for 30 min. Then the tubes that contained the metal nanoparticles were centrifuged at 3,000 rpm for 20 mins. The supernatants were collected to determine the concentration of cobalt or titanium ion by inductively coupled plasma-atomic emission spectrometry (ICP-AES). The results are shown in Table 2.

Chemicals and reagents

2′, 7′-dichlorodihydrofluorescein diacetate (H_2-DCFDA) was obtained from Molecular Probes (Eugene, OR), catalase (CAT) from MP Biomedicals (Solon, OH), N-acetyl-L(+)-cysteine (NAC) from Fisher (Fair Lawn, NJ). The ATM inhibitor KU-55933 was purchased from Calbiochem (San Diego, CA). Monoclonal anti-phospho-ATM and anti-ATM, and polyclonal anti-phospho-p53 (Ser 15) antibodies were purchased from Cell Signaling Technology (Beverly, MA), HRP-conjugated anti-mouse IgG, polyclonal anti-Rad51 and monoclonal anti-p53 (DO-1) antibodies from Santa Cruz Biotechnology (Santa Cruz, CA), monoclonal anti-γH2AX antibody from Millipore (Billerica, MA), monoclonal anti-β-actin antibody from Sigma-Aldrich (Saint Louis, MO). HRP-conjugated goat anti-rabbit IgG was purchased from CHEMICON (Temecula, CA) and rhodamine red-X goat anti-mouse from

Invitrogen (Carlsbad, CA). The ECL™ Western Blotting Detection Reagents was purchased from GE Healthcare, Amersham™ (Buckinghamshire, UK).

Cell culture and treatment

The human lung epithelial cell lines A549 was obtained from American Type Culture Collection (ATCC) (Rockville, MD). A549 cells were cultured as a monolayer in Ham's F-12 medium (Mediatech, Inc., Manassas, VA) supplemented with 10% heat-inactivated fetal bovine serum (Mediatech Inc.), 100 U/ml penicillin, and 100 μg/ml streptomycin (Mediatech Inc.) and maintained in an incubator with a humidified atmosphere of 5% CO_2 at 37°C.

In vitro cytotoxicity assay

The cytotoxicity of metal nanoparticles was analyzed by both an *in vitro* cytotoxicity assay kit (Sulforhodamine B Based, Sigma-Aldrich, St Louis, MO) (SRB assay) and the AlamarBlue™ assay (AbD Serotex, Oxford, UK) according to the manufacturer's directions. Briefly, 5×10^3 A549 cells were seeded into each well of 96-well plates and were allowed to attach to the growth surface by culturing overnight. Cells were then treated with different concentrations (0, 2.5, 5, 10, 15, 20 and 40 μg/ml) of Nano-Co or Nano-TiO_2 in a total volume of 200 μl per well for 24 h. For SRB assay, the adherent cells were fixed in situ with 50% TCA, incubated at 4°C, then washed, and dyed with SRB. The incorporated dye was solubilized in 10 mM Tris base. The absorbance at 565 nm was recorded using a multi-detection microplate reader (Synergy HT, BioTek, Vermont, USA). The background absorbance at 690 nm was measured and subtracted from the measurement at 565 nm. The cell viability was expressed as the percentage of the control which was without treatment. Another method, AlamarBlue™ assay, is a colorimetric/fluorometric method for determining the number of metabolically active cells through oxidation-reduction indicator. This method was performed as in our previous study.[42]

Uptake of metal nanoparticles by inductively coupled plasma mass spectrometry (ICP-MS)

The uptake of metal nanoparticles by A549 cells was measured by using ICP-MS as reported previously.[44–45] In brief, 80% confluent A549 cells were exposed to 5 and 15 μg/ml of Nano-Co and Nano-TiO_2 for 12 hr, washed with PBS and collected. The cell pellet was resuspended in 1.0 ml PBS and the number of cells was counted by using a hemacytometer. The cells were treated with 3 ml of 1% HNO_3 aqueous solution, then heated to 80°C for 3 h to dissolve cell content. The PBS solution without cells underwent all the treatment processes, and was used as a blank control for ICP-MS. The concentrations of Ti and Co were determined by ICP-MS (DRCII, Perkin Elmer).

Intracellular ROS measurement

Intracellular ROS production was measured using the fluorescent probe H_2-DCFDA as described previously.[41–44] H_2-DCFDA is nonfluorescent and cell permeant. It can rapidly diffuse through the cell membrane and is hydrolyzed by intracellular esterases to an oxidative sensitive form, dichlorodihydrofluorescein (H_2-DCF). This serves as a substrate for intracellular oxidants to generate highly fluorescent DCF, with a fluorescent intensity proportional to intracellular ROS. A 20 mM stock solution of H_2-DCFDA was prepared in 100% ethanol and stored at −20°C in the dark. After cells were seeded into a 96-well plate and allowed to attach to the growth surface by culturing overnight, cells were incubated for 2 h with H_2-DCFDA at 37°C in the dark by adding it directly to the cell culture medium to make a final concentration of 5 μM. Then cells were treated with 0, 2.5, 5, 10 and 15 μg/ml of Nano-Co or Nano-TiO_2 for 12 h. Cells without metal nanoparticle exposure were used as control. Fluorescence was determined at 485 nm excitation and 528 nm emission by multi-

detection microplate reader (Synergy HT, BioTek, Vermont). Cell fluorescence without the addition of H_2-DCFDA was used as background fluorescence level and subtracted from the sample fluorescence level. Results, in arbitrary fluorescence units (AFU), were expressed according to the ratio [(AFU in treated cells)/(AFU in control cells)] × 100.

To examine the role of antioxidants on ROS generation in A549 cells after exposure to Nano-Co, A549 cells were pre-treated with ROS scavengers or inhibitors such as NAC (10 mM) or CAT (2000 U/ml) for 2 h, then cells were preloaded with 5 μM H_2-DCFDA for another 2 h prior to exposure to 15 μg/ml of Nano-Co for 12 h. Fluorescence values were measured as described above.

Alkaline comet assay

DNA damage in A549 cells with exposure to metal nanoparticles was examined by CometAssay™ Reagent Kit (Trevigen, Gaithersburg, MD) according to the manufacturer's instructions. Briefly, A549 cells were seeded in 25 cm^2 flasks (5×10^5 cells per flask) and exposed to 0, 5 and 15 μg/ml of Nano-Co or Nano-TiO_2 for 12 h. After treatment, the cells were re-suspended at a concentration of $1\times 10_5$ cells per ml of cold 1×PBS. The individual cell was embedded in low melting point agarose on a slide glass. Samples were then immersed in a lysis solution (2.5 M NaCl, 100 mM EDTA, 10 mM Tris-HCl, 1% Triton X-100, and 10% dimethyl sulfoxide, pH 10) for 1 h at 4 °C, followed by treatment with fresh alkaline solution (1 mM EDTA, 300 mM NaOH, pH13.5) for 1 h at 4°C to allow the DNA double helix to denature and the nucleoid to become single strand. Electrophoresis was performed in a horizontal electrophoresis unit filled with the fresh alkaline solution at 300 mA for 30 min. The agarose gels on the slides were then neutralized with 400 mM Tris–HCl (pH 7.4), fixed with 100% ethanol, stained with SYBR Green I and scored using a fluorescence microscope (Nikon, Oberkochen, Japan) at 400X magnification. The olive tail moment parameter was used to quantify the DNA damage as previously reported,[28] which was calculated as the tail length multiplied by the fraction of DNA in the comet tail.

Immunofluorescence staining of γ-H2AX foci formation

A549 cells were seeded at 1×10^5 cells/well in 2-well LAB-TEK® II chamber slides (Nalge Nunc International, IL) and incubated overnight prior to treatment. In the dose-response study, the cells were treated with 0, 5 and 15 μg/ml of Nano-Co or Nano-TiO_2 for 6 h. In the time-response study, the cells were treated with 15 μg/ml of Nano-Co or Nano-TiO_2 for 0, 1, 3, 6, and 12, respectively. After treatment, the cells were washed with 1×PBS, fixed with ice-cold methanol/acetone solution (1:1) and incubated with a 1:1000 dilution of anti-H2AX antibody (γ-H2AX) at 4°C overnight. Cells were then incubated with a 1:500 dilution of a goat anti-mouse secondary antibody conjugated with the fluorochrome Rhodamine Red-X (Molecular Probes) for 1 h at room temperature and stained with 4′,6-diamidino-2-phenylindole dihydrochloride (DAPI, 0.1μg/ml) (AnaSpec.Inc, CA) for 5 min. The slides were washed and then visualized under fluorescence microscope (Nikon, Oberkochen, Japan). γ-H2AX foci were counted in 100 cells per time or dose point and the results were expressed as the % of γ-H2AX positive cells from three independent experiments.

Protein extraction and western blot analysis

Cells treated with Nano-Co or Nano-TiO_2 were collected, and cytosolic proteins were prepared using RIPA Lysis Buffer Kit (Santa Cruz) according to the manufacturer's instruction. Proteins were quantified by the Bradford method. 100 μg of protein per sample was denatured at 100°C for 5 min and separated on 7.5%~12% SDS-PAGE. After the protein was transferred onto polyvinylidene difluoride (PVDF) membranes (Millipore, Billerica, MA), the nonspecific binding sites were blocked with 5% skim milk in TBST (50 mM Tris-HCl, 140 mM NaCl, 0.05% Tween 20, pH 7.2) for 2 h at room temperature. Then

the membrane was incubated with the primary antibody at 4°C overnight, followed by incubating with the second antibody for one hour and developing by using ECL™ Western Blotting Detection Reagents. Densitometric analyses were performed to quantify Western blotting signals by using NIH Image J software. The density of each band was normalized to that of β-actin. For phospho-p53, p53, phospho-ATM and ATM testing, nuclear extracts were prepared using NE-PER® Nuclear Extraction Reagent (Pierce, Rockford, IL) and equal protein loading was verified by Coomassie Brilliant Blue staining.

Statistical analysis

Data were expressed as the mean ± SE. For dose-response studies, differences among groups were evaluated with two-way analysis of variance; if the F-value was significant, groups were then compared at each dose by one-way analysis of variance (ANOVA) followed by Dunnett's t-test. If a *p* value was less than 0.05, a difference was considered statistically significant. Statistical analyses were carried out using Sigma Stat (Jandel Scientific, San Raphael, CA).

Acknowledgments

Some of research described in this article was conducted under contract to the Health Effects Institute (HEI), an organization jointly founded by the United States Environmental Protection Agency (EPA) (Assistance Award No. R-8281101) and certain motor vehicle and engine manufacturers. The contents of this article do not necessarily reflect the views of HEI, or its sponsors, nor do they necessarily reflect the views and policies of the EPA or motor vehicle and engine manufacturers.

Funding Support

This work was partly supported by the American Lung Association (RG-872-N), American Heart Association (086576D), KSEF-1686-RED-11, Health Effects Institute (4751-RFA-052/06-12), Basic Award of Clinical & Translational Sciences Pilot Grant Program from UofL (20018), an Intramural Research Incentive Grants (50753) from UofL, NIESH T32-ES011564 and ES01443.

Abbreviations

ATM	ataxia telangiectasia mutatant
CAT	catalase
H_2-DCFDA	2', 7'-dichlorodihydrofluorescein diacetate
DAPI	4′,6-diamidino-2-phenylindole dihydrochloride
DSBs	double-strand breaks
Nano-Co	nano-sized cobalt
Nano-TiO_2	nano-sized titanium dioxide
ROS	reactive oxygen species
NAC	N-acetyl-L(+)-cysteine

References

1. Chow JC, Watson JG, Savage N, Solomon CJ, Cheng YS, McMurry PH, Corey LM, Bruce GM, Pleus RC, Biswas P, Wu CY. Nanoparticles and the Environment. J. Air and Waste Manage. Associ. 2005; 55:1411–1417.
2. Colvin VL. The potential environmental impact of engineered nanomateroials. Nat. Biotechnol. 2003; 21:1166–1170. [PubMed: 14520401]

3. Owen R, Depledge M. Nanotechnology and the environment: risk and rewards. Marine Pollution Bulletin. 2005; 50:609–612. [PubMed: 15919099]
4. Oberdorster G, Oberdoster E, Oberdorster L. Nanotoxicology: An emerging discipline evolving from studies of ultrafine particles. Environ. Health Perspect. 2005; 113:823–839. [PubMed: 16002369]
5. Xia T, Li N, Nel AE. Potential health impact of nanoparticles. Annu. Rev. Public Health. 2009; 30:137–150. [PubMed: 19705557]
6. Valko M, Morris H, Cronin MTD. Metal, toxicity, and oxidative stress. Curr. Med. Chem. 2005; 12:1161–1208. [PubMed: 15892631]
7. Valko M, Rhodes CJ, Moncol J, Izakovic M, Mazur M. Free radicals, metals and antioxidants in oxidative stress-induced cancer. Chem. Biol. Interact. 2006; 160:1–40. [PubMed: 16430879]
8. Gonealez Lison D, Krisch-Volders M. Gneotoxicity of engineered nanomaterials: a critical review. Nanotoxicology. 2008; 2:252–273.
9. Landsiedel R, Kapp MD, Schulz M, Wiench K, Oesch F. Genotoxicity investigation on nanomaterials: methods, preparation and characterization of test material, potential artifacts and limitations-many questions, some answers. Mutat. Res. 2009; 681:541–528.
10. Wang K, Xu JJ, Chen HY. A novel glucose biosensor based on the nanoscaled cobalt phthalocyanine glucose oxidase biocomposite. Biosens. Bioelectron. 2005; 20:1388–1396. [PubMed: 15590294]
11. Yang MH, Jiang JH, Yang YH, Chen XH, Shen GL, Yu RQ. Carbon nanotube/cobalt hexacyanoferrate nanoparticle-biopolymer system for the fabrication of biosensors. Biosens. Bioelectron. 2006; 21:1791–1797. [PubMed: 16230002]
12. Galanis A, Karapetsas A, Sandaltzopoulos R. Metal-induced carcinogenesis, oxidative stress and hypoxia signaling. Mutat. Res. 2009; 674:31–35. [PubMed: 19022395]
13. Pulido MD, Parrish AR. Metal-induced apoptosis: mechanism. Mutat. Res. 2003; 533:227–241. [PubMed: 14643423]
14. Risom L, Moller P, Loft S. Oxidative stress-induced DNA damage by particulate air pollution. Mutat. Res. 2005; 592:119–137. [PubMed: 16085126]
15. Barchowsky A, O'Hara KA. Metal-induced cell signaling and gene activation in lung disease. Free Radic. Biol. Med. 2003; 34:1130–1135. [PubMed: 12706493]
16. Banin S, Moyal L, Shieh S, Taya Y, Anderson CW, Chessa L, Smorodinsky NI, Prives C, Reiss Y, Shiloh Y, Ziv Y. Enhanced phosphorylation of p53 by ATM in response to DNA damage. Science. 1998; 81:1674–1677. [PubMed: 9733514]
17. Suzuki K, Inageda K, Nishitai G, Matsuoka M. Phosphorylation of p53 at serine 15 A549 pulmonary epithelail cells exposure to vanadate: involvement of ATM pathway. Toxicol. and Appl. Pharmacol. 2007; 220:83–91. [PubMed: 17292432]
18. Vousden KH, Lane DP. P53 in health and disease. Nat. Rev. Mol. Cell Biol. 2007; 8:275–283. [PubMed: 17380161]
19. Zhao H, Traganos F, Darzynkiewicz Z. Phosphorylation p53 on Ser 15 during cell cycle caused by Topo I and Topo II inhibitor in relation to ATM and Chk2 activation. Cell Cycle. 2008; 7:3048–3055. [PubMed: 18802408]
20. Lavin MF, Kozlov S. ATM activation and DAN damage response. Cell Cycle. 2007; 6:931–942. [PubMed: 17457059]
21. Tanaka T, Halicka XD, Huang X, Traganos F, Darzynkiewicz Z. Constitutive histone H2AX phosphorylation and ATM activation, the reporters of DNA damage by endogenous oxidants. Cell Cycle. 2006; 5:1940–1945. [PubMed: 16940754]
22. Kurz EU, Lees-Miller SP. DAN damage-induced activation of ATM and ATM-dependent signaling pathways. DNA Repair. 2004; 3:889–900. [PubMed: 15279774]
23. De Boeck M, Krisch-Volders M, Lison D. Cobalt and antimony: genotoxicity and carcinogenicity. Mutat. Res. 2003; 533:135–152. [PubMed: 14643417]
24. De Boeck M, Hoet P, Lombaert N, Nemery B, Kirsch-Volders M, Lison D. *In vivo* genotoxicity of hard metal dust: induction of micronuclei in rat type II epithelial lung cells. Carcinogenesis. 24:1793–1800. [PubMed: 12949052]

25. Colognato R, Bonelli A, Ponti J, Farina M, Bergamaschi E, Sabbioni E, Migliore L. Comparative genotoxicity of cobalt nanoparticles and ions on human peripheral leukocytes *in vitro*. Mutagenesis. 2008; 23:377–382. [PubMed: 18504271]
26. Hoeijmakers JH. Genome maintenance mechanisms for preventing cancer. Nature. 2001; 411:366–374. [PubMed: 11357144]
27. IARC working group. Cobalt and cobalt compounds. Vol. Vol. 52. Lyon: IARC; 1992. In: IARC monographs on the evaluation of the carcinogenic risk of chemicals to man; p. 263-473.
28. Karlsson HL. The comet assay in nanotoxicology research. Anal. Bioanal. Chem. 2010; 398:651–666. [PubMed: 20640410]
29. Ponti J, Sabbioni E, Munaro B, Broggi F, Marmorato P, Franchini F, Colognato R, Rossi F. Genotoxicity and morphological transformation induced by cobalt nanoparticles and cobalt chloride: an *in vitro*. study in Balb/3T3 mouse fibroblasts. Mutagenesis. 2009; 24:439–445.
30. Lison D, De Boeck M, Verougstraete V, Kirsch-Volders M. Update on the genotoxicity and carcinogenicity of cobalt compounds. Occup. Environ. Med. 2001; 58:619–625. [PubMed: 11555681]
31. Sedelnikova OA, Pilch DR, Redon C, Bonner WM. Histone H2AX in DNA damage and repair. Cancer Biol. Ther. 2003; 2:233–235. [PubMed: 12878854]
32. Mah LJ, El-Osta A, Karagiannis TC. GammaH2AX as a molecular marker of aging and disease. Epigenetics. 2010; 5:129–136. [PubMed: 20150765]
33. Mah LJ, El-Osta A, Karagiannis TC. GammaH2AX: a sensitive molecular marker of DNA damage and repair. Leukemia. 2010; 24:679–686. [PubMed: 20130602]
34. Paull TT, Rogakou EP, Yamazaki V, Kirchgessner CU, Gellert M, Bonner WM. A critical role for histone H2AX in recruitment of repair factors to nuclear foci after DNA damage. Curr. Biol. 2000; 10:886–895. [PubMed: 10959836]
35. Shieh SY, Ikeda M, Taya Y, Prives C. DNA damage-induced phosphorylation of p53 alleviates inhibition by MDM2. Cell. 1997; 3191:325–334. [PubMed: 9363941]
36. Siliciano JD, Canman CE, Taya Y, Sakaguchi K, Appella E, Kastan MB. DNA damage induces phosphorylation of the amino terminus of p53. Genes. Dev. 1997; 11:3471–3481. [PubMed: 9407038]
37. Ismail IH, Nystrom S, Nygren J, Hammarsten O. Activation of ataxia telangiectasia mutated by DNA strand break-inducing agents correlates closely with the number of DNA double strand breaks. J. Biol. Chem. 2005; 280:4649–4655. [PubMed: 15546858]
38. Xie H, Wise SS, Holmes AL, Xu B, Wakeman TP, Pelsue SC, Singh NP, Wise JP Sr. Carcinogenic lead chromate induces DNA double-strand breaks in human lung cells. Mutat. Res. 2005; 586:160–172. [PubMed: 16112599]
39. Canman CE, Lim DS, Cimprich KA, Taya Y, Tamai K, Sakaguchi K, Appella E, Kastan MB, Siliciano JD. Activation of the ATM kinase by ionizing radiation and phosphorylation of p53. Science. 1998; 281:1677–1679. [PubMed: 9733515]
40. Kyono H, Kusaka Y, Homma K, Kubota H, Endo-ichikawa Y. Reversible lung lesions in rats due to short-term exposure to ultrafine cobalt particles. Ind. Health. 1992; 30:103–118. [PubMed: 1301410]
41. Wan R, Mo Y, Chien S, Li Y, Li Y, Tollerud DJ, Zhang Q. The role of hypoxia inducible factor-1α in MMP-2 and MMP-9 production by human monocytes exposed to nickel nanoparticles. Nanotoxicology. 2011; 5(4):568–582. [PubMed: 21401309]
42. Yu M, Mo Y, Wan R, Chien S, Zhang X, Zhang Q. Regulation of plasminogen activator inhibitor-1 expression in endothelial cells with exposure to metal nanoparticles. Toxicol. Lette. 2010; 195:82–89.
43. Mo Y, Wan R, Wang J, Chien S, Tollerud DJ, Zhang Q. Diabetes is associated with increased sensitivity of alveolar macrophages to urban particulate matter exposure. Toxicology. 2009; 262:130–137. [PubMed: 19505525]
44. Wan R, Mo Y, Zhang X, Chien S, Tollerud DJ, Zhang Q. Matrix metalloproteinase-2 and-9 are induced differently by metal nanoparticles in human monocytes: the role of oxidative stress and protein tyrosine kinase activation. Toxicol. and Appl. Pharmacol. 2008; 233:276–285. [PubMed: 18835569]

45. Gojova A, Guo B, Kota RS, Rutledge JC, Kennedy IM, Barakat AI. Induction of inflammation in vascular endothelial cells by metal oxide nanoparticles: effect of particle composition. Environ. Health Perspect. 2007; 115:403–409. [PubMed: 17431490]

46. Cho EC, Zhang Q, Xia Y. The effect of sedimentation and diffusion on cellular uptake of gold nanoparticles. Nat Nanotechnol. 2011; 6(6):385–391. [PubMed: 21516092]

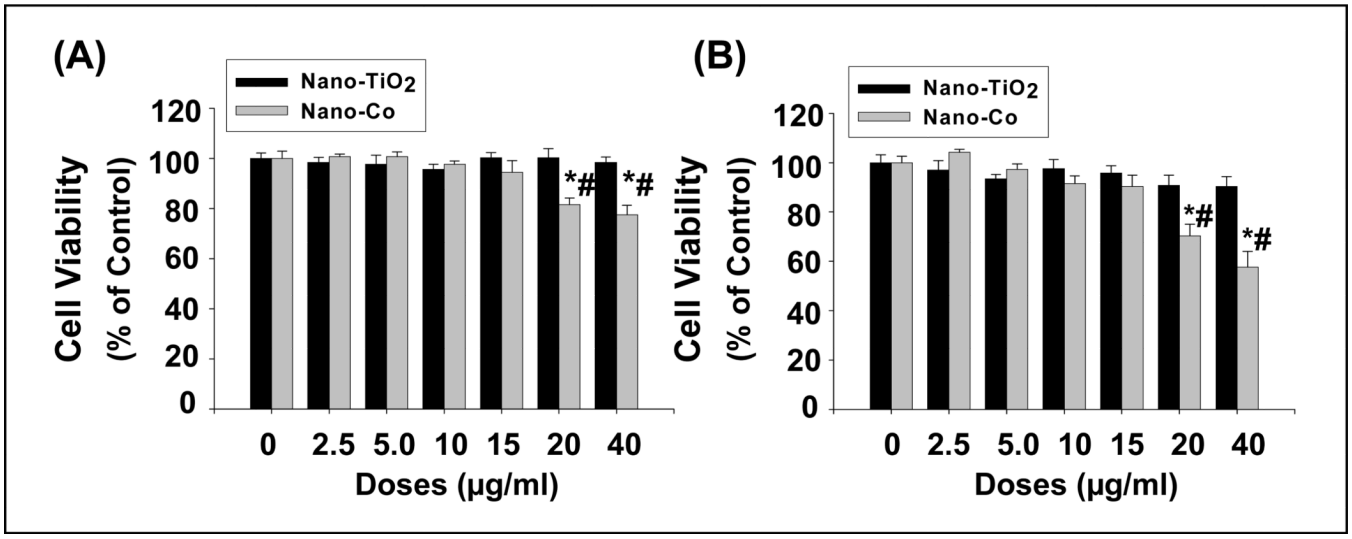

Fig. 1. Cytotoxicity of Nano-Co and Nano-TiO_2 on A549 cells

A549 cells were treated with different doses of Nano-Co or Nano-TiO_2 for 24h, and cytotoxicity was determined by both SRB assay (A) and AlamarBlue™ assay (B). A549 cells without treatment were used as controls. Values are mean ± SE of six experiments. * Significant difference from the control, $p < 0.05$; # Significant difference from the same dose of Nano-TiO_2-treated group, $p < 0.05$.

Fig. 2A

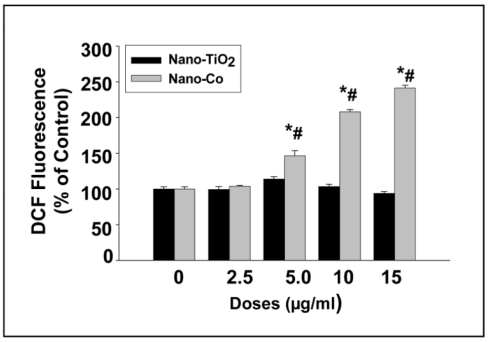

Fig. 2B

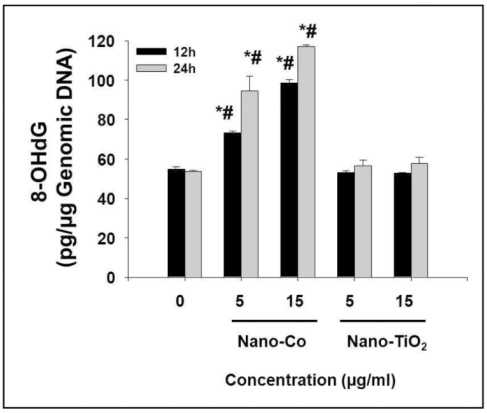

Fig. 2C

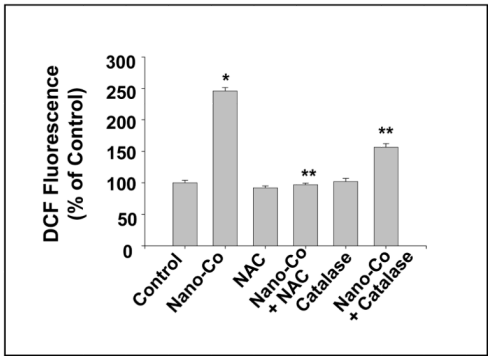

Fig. 2. Effects of Nano-Co and Nano-TiO_2 exposure on ROS generation (A) and 8-OHdG levels (b) in A549 cells and the effects of ROS scavengers or inhibitors on Nano-Co-induced ROS generation (C)

A549 cells were pretreated with 5 μM H_2-DCFDA for 2 h prior to exposure to Nano-TiO_2 or Nano-Co for 12 h (A). A549 cells were treated with Nano-Co or Nano-TiO_2 for 12h and 24h, respectively. 8-OHdG level was assayed by OxiSelect™ Oxidative DNA Damage ELISA Kit. (B). For antioxidant experiments, NAC or catalase was added 2 h prior to adding H_2-DCFDA and Nano-Co (C). A549 cells without treatment were used as controls. Values are mean ± SE of six experiments. * Significant difference compared with the

control, $p < 0.05$; # significant difference from the same dose of Nano-TiO_2-treated group, $p < 0.05$; ** significant difference as compared with Nano-Co alone, $p < 0.05$.

Fig. 3A

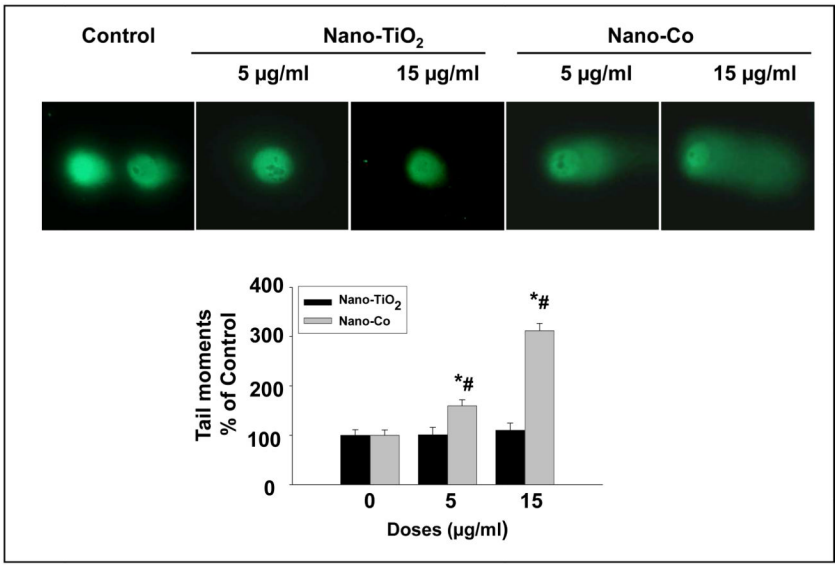

Fig. 3B

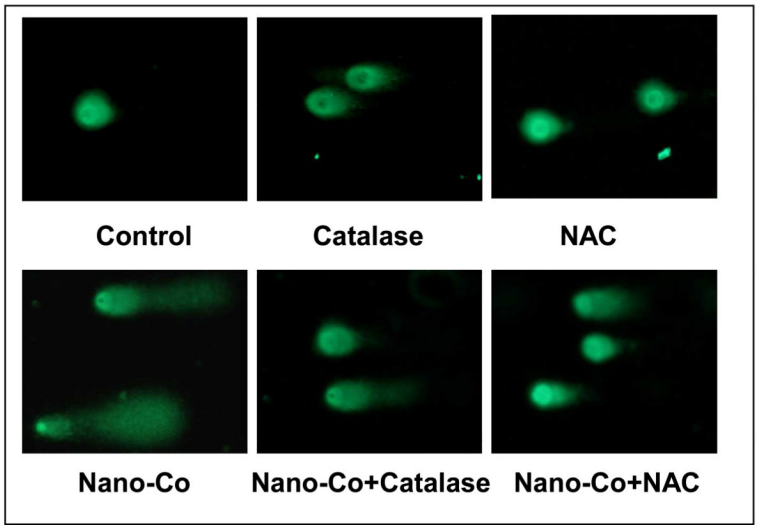

Fig. 3. Effects of Nano-Co or Nano-TiO_2 exposure on DNA double-strand breaks (DSBs) in A549 cells (A) and the effects of ROS scavengers or inhibitors on Nano-Co-induced DSBs in A549 cells (B)

A549 cells were treated with 0, 5 and 15 μg/ml of Nano-Co or Nano-TiO_2 for 12h, and DSBs was determined by alkaline single-cell gel electrophoresis (Comet) assay and the tail moment was used as an index of damage (A). Values are mean ± SE of three independent experiments. Three slides per concentration and 100 comets per slide were analyzed in each experiment. For antioxidant experiments, catalase (2,000 U/ml) or NAC (10 mM) was added 2 h prior to adding 15 μg/ml Nano-Co for another 12 h and Comet assay was performed (B).

* Significant difference as compared with the control, $p < 0.05$; # Significant difference as compared with the same dose of Nano-TiO_2-treated group, $p < 0.05$.

Fig. 4A

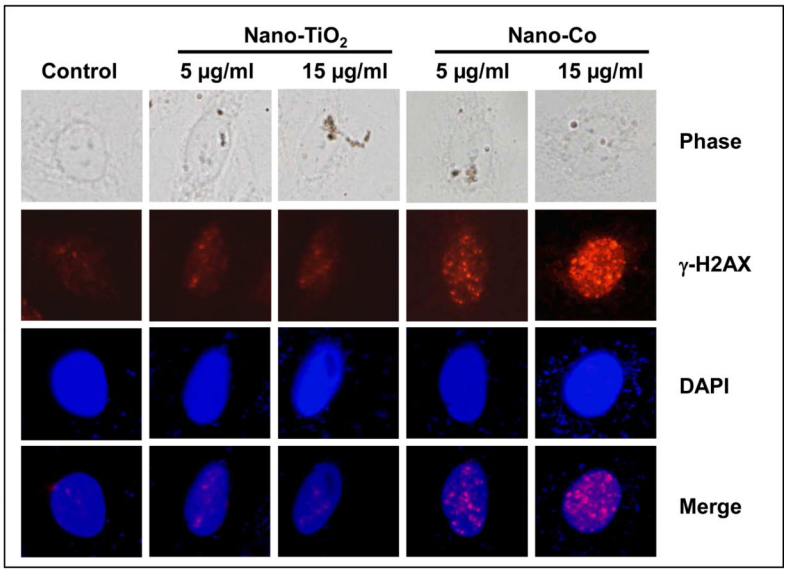

Fig. 4B

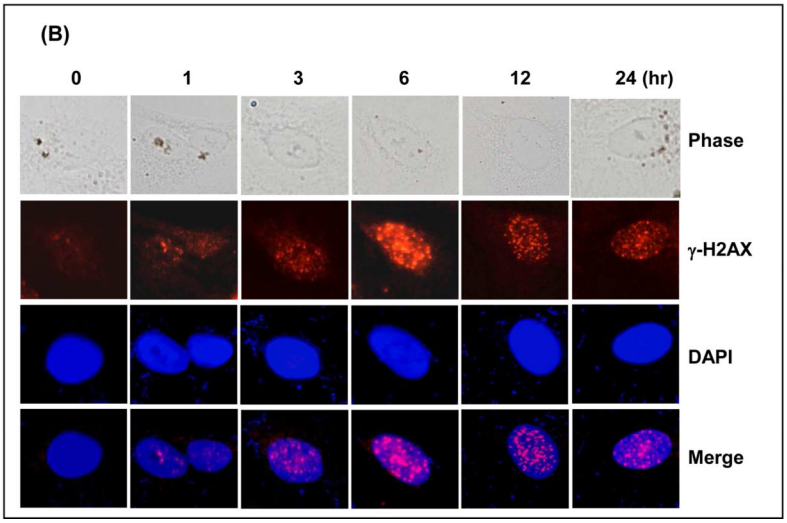

Fig. 4. Dose- and time- response increase in γ-H2AX foci formation in A549 cells exposed to Nano-Co

A549 cells were exposed to Nano-Co or Nano-TiO_2 (5 and 15 μg/ml) for 6 h (A) or exposed to 15 μg/ml of Nano-Co for 1, 3, 6, 12, and 24 h (B). Cells without treatment were used as controls. DAPI (blue) is used as a marker for DNA and stains the whole nucleus of a cell. The red γ-H2AX-specific foci reproduce as pink in the merged images due to color overlay. Magnification is 1000×.

Fig. 5A

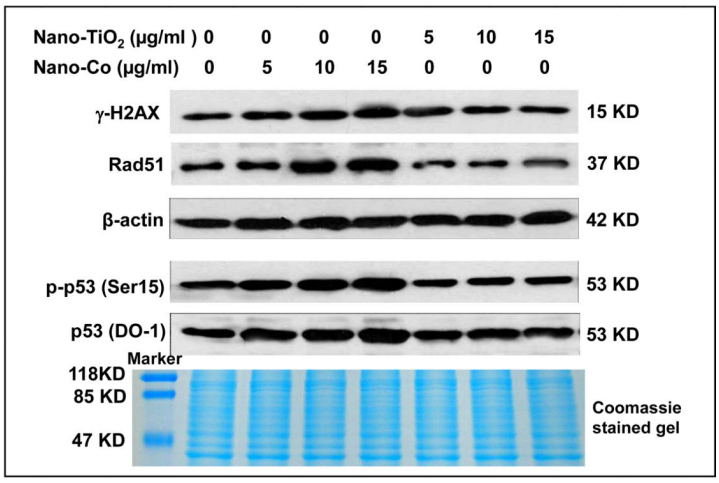

Fig. 5B

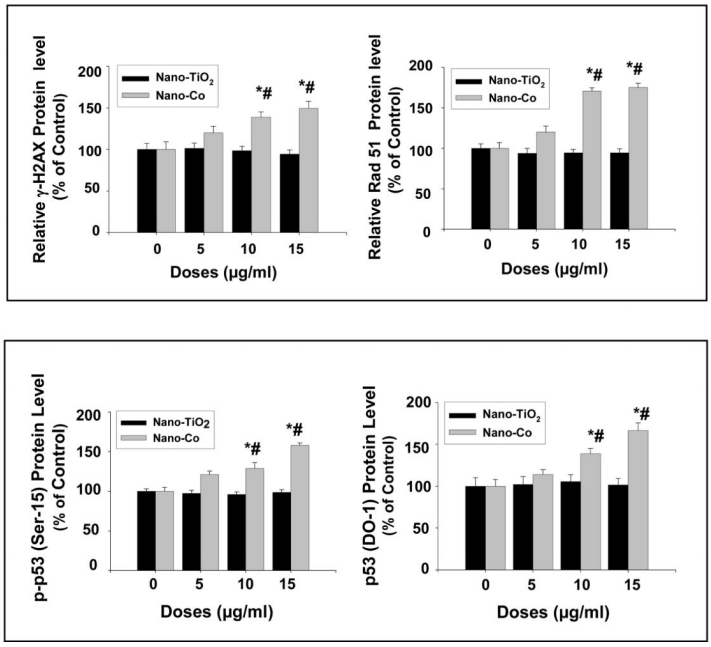

Fig. 5C

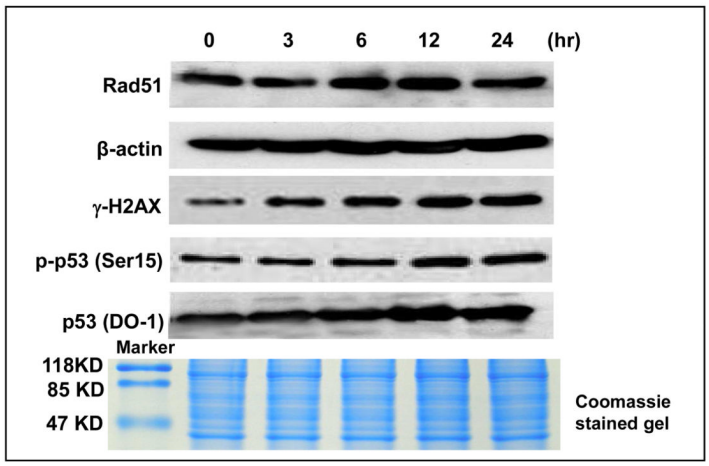

Fig. 5D

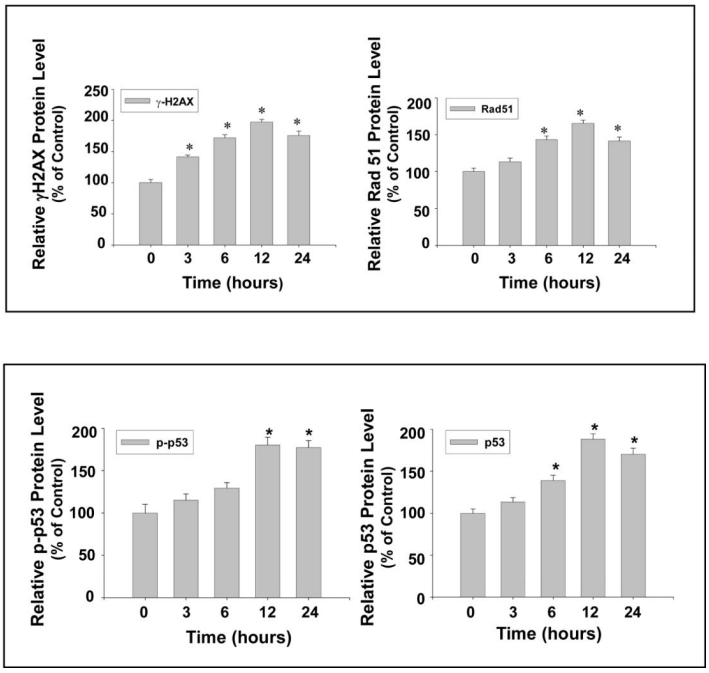

Fig. 5. Dose- and time- response induction of γ-H2AX at Ser 139, Rad51, p-p53 at Ser 15 and p53 expression in A549 cells exposed to Nano-Co

Cells were treated with 0, 5, 10 and 15 μg/ml of Nano-Co or Nano-TiO_2 for 12 h (A & B) or with 15 μg/ml of Nano-Co for 0, 3, 6, 12 and 24 h (C & D). Cells without treatment were used as control. Cytosolic protein (for Rad51 and β-actin) or nuclear protein (for γ-H2AX, p-p53 and p53) was prepared for Western blot. A and C were results of a signal Western blot experiment, while B and D were normalized band densitometry readings averaged from 3 independent experiments ± SE of Western results. β-actin or Coomassie blue stained gel was used for verification of equality of lane loading. * Significant difference as compared with

the control, $p < 0.05$; # Significant difference as compared with the same dose of Nano-TiO_2-treated group, $p < 0.05$.

Fig. 6A

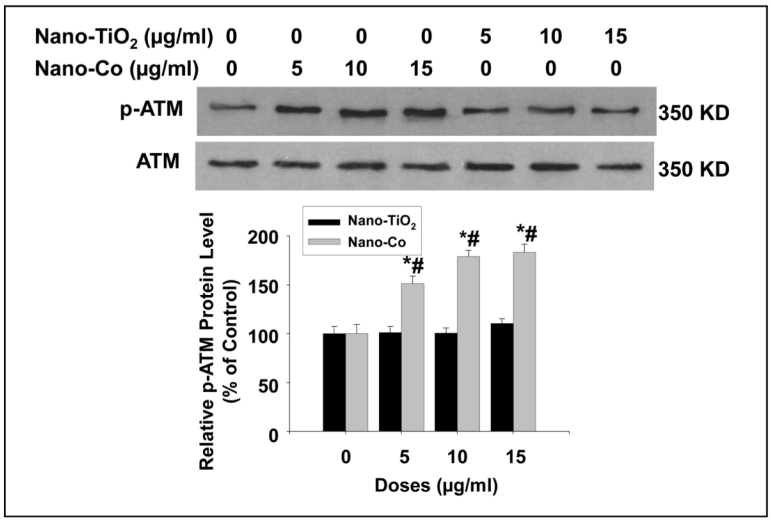

Fig. 6B

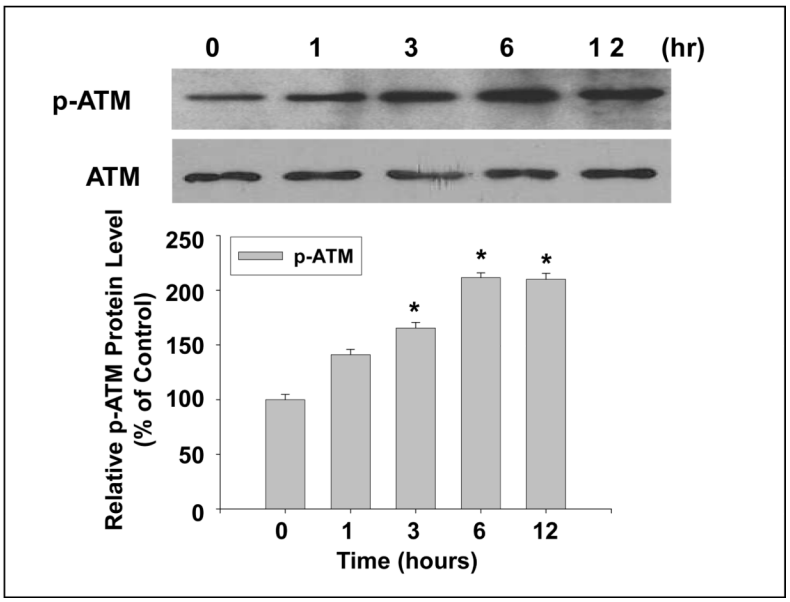

Fig. 6. Dose- and time- response induction of phosphorylation of ATM at Ser 1981 in A549 cells exposed to Nano-Co or Nano-TiO_2

A549 cells were treated with 0, 5, 10 and 15 μg/ml of Nano-Co or Nano-TiO_2 for 6 h (A) or with 15 μg/ml of Nano-Co for 0, 1, 3, 6 and 12 h (B). Cells without treatment were used as control. Nuclear protein was extracted for Western blot. Total ATM was used for verification of equality of lane loading. * Significant difference as compared with the control, $p < 0.05$; # Significant difference as compared with the same dose of Nano-TiO_2-treated group, $p < 0.05$.

Fig. 7A

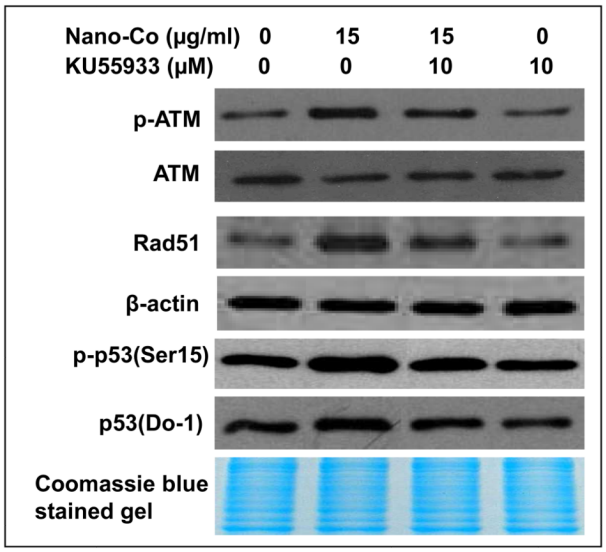

Fig. 7B

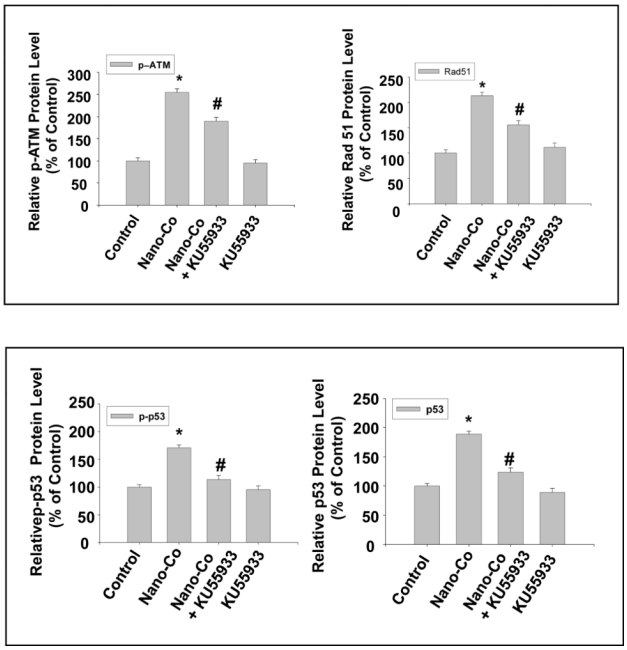

Fig. 7. Effects of the specific ATM inhibitor, KU55933, on Nano-Co-induced increased phosphorylation of p53 and ATM, and increased expression of Rad51 and p53

A549 cells were pre-treated with an ATM inhibitor, KU55933 (10 μM) for 1 h prior to treatment with Nano-Co (15 μg/ml) for 12 h. Cytosolic protein (for Rad51 and β-actin) or nuclear protein (for p-ATM, ATM, p-p53 and p53) was extracted for Western blot. Cells without any treatments were used as controls. A is the result of a single experiment. B is normalized band densitometry reading averaged from three independent experiments ± SE of Western blot results. β-actin or Coomassie blue stained gel was used to verify the equality of lane loading. * Significant difference as compared with the control, $p < 0.05$; # Significant difference as compared with the Nano-Co-treated group, $p < 0.05$.

Fig. 8A

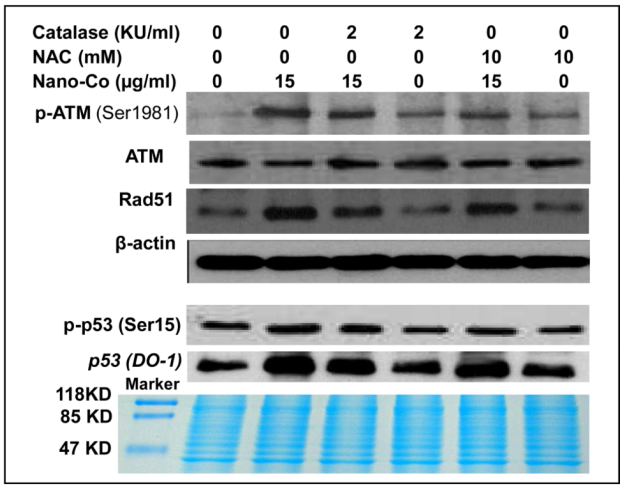

Fig. 8B

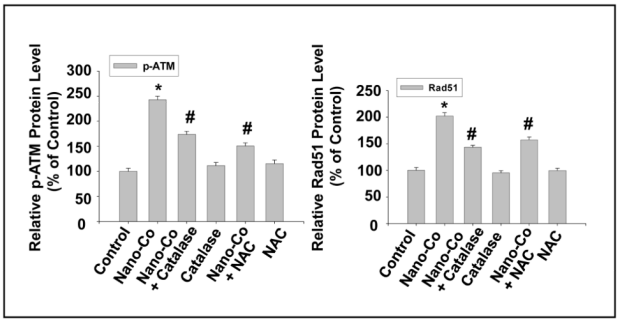

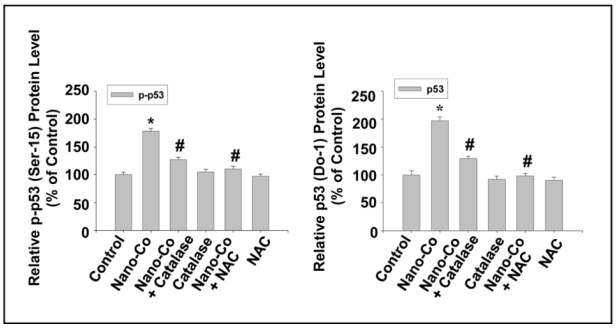

Fig. 8. Effects of ROS scavengers or inhibitors on Nano-Co-induced phosphorylation of ATM and p53, and increased expression of Rad51 and p53

A549 cells were pre-treated with Catalase (2,000 U/ml) or NAC (10 mM) for 2 h prior to exposure to 15 μg/ml of Nano-Co for another 12 h. Cells without treatment were used as controls. Cytosolic protein (for Rad51 and β-actin) or nuclear protein (for p-ATM, ATM, p-p53 and p53) was prepared for Western blot. Total ATM (for p-ATM), β-actin (for Rad51) or Coomassie blue stained gel (for p-p53 and p53) was used to verify the equality of lane loading. A is the result of a single experiment. B is normalized band densitometry reading averaged from three independent experiments ± SE of Western blot results. * Significant

difference as compared with the control, $p < 0.05$; # Significant difference as compared with the Nano-Co-treated group, $p < 0.05$.

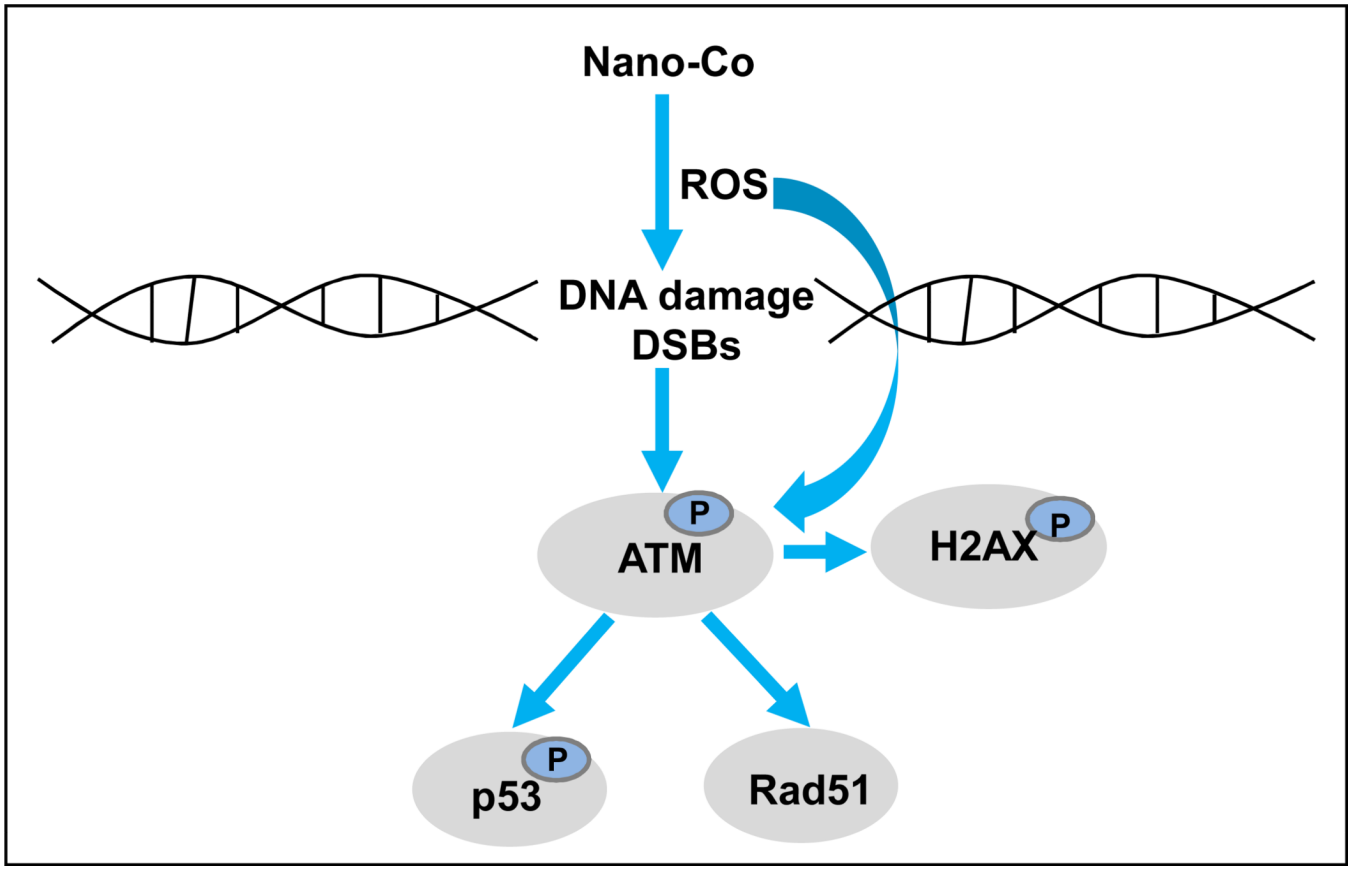

Fig. 9. A schematic diagram of the signaling pathways that may be involved in Nano-Co-induced DNA damage

Exposure of A549 cells to Nano-Co caused oxidative stress, which may further result in DNA DSBs and activate ATM. Increased phosphorylation of ATM may mediate the phosphorylation of p53 and H2AX and upregulation of Rad51 expression.

Table 1

Characterization of metal nanoparticles

Metal	Particle size in powder (Diameter) (nm, average)	TEM (nm) Diameter	DLS (nm) Diameter	Specific surface area (m2/g)	Phase composition
Nano-Co	20	10–40	260	47.9	Co (85–90%) Co_3O_4 (10–15%)
Nano-TiO_2	28	10–60	280	45.0	Anatase (90%) Rutile (10%)

Table 2

Solubility of metal nanoparticles in PBS and F-12 medium

Metal	PBS (ppm)	F-12 medium (ppm)
Nano-Co	10.81±0.62	45.35±1.68
Nano-TiO_2	<1.00	<1.00